ORGANOMETALLICS

Article

pubs.acs.org/Organometallics

Nickel Catalysts for the Dehydrative Decarbonylation of Carboxylic Acids to Alkenes

Alex John,[†,§] Maria O. Miranda,[†,§] Keying Ding,[†,§] Büsra Dereli,[†] Manuel A. Ortuño,[†] Anne M. LaPointe,[*,‡] Geoffrey W. Coates,[*,‡] Christopher J. Cramer,[*,†] and William B. Tolman[*,†]

[†]Department of Chemistry, Center for Sustainable Polymers, Chemical Theory Center, and Minnesota Supercomputing Institute, University of Minnesota, 207 Pleasant Street SE, Minneapolis, Minnesota 55455, United States

[‡]Department of Chemistry and Chemical Biology, Baker Laboratory, Cornell University, Ithaca, New York 14853-1301, United States

Supporting Information

ABSTRACT: Combining high-throughput experimentation with conventional experiments expedited discovery of new first-row nickel catalysts for the dehydrative decarbonylation of the bioderived substrates hydrocinnamic acid and fatty acids to their corresponding alkenes. Conventional experiments using a continuous distillation process (180 °C) revealed that catalysts composed of Ni^{II} or Ni^{0} precursors (NiI_2, $Ni(PPh_3)_4$) and simple aryl phosphine ligands were the most active. In the reactions with fatty acids, the nature of the added phosphine influenced the selectivity for α-alkene, which reached a maximum value of 94%. Mechanistic studies of the hydrocinnamic reaction using $Ni(PPh_3)_4$ as catalyst implicate a facile first turnover to produce styrene at room temperature, but deactivation of the Ni(0) catalyst by CO poisoning occurs subsequently, as evidenced by the formation of $Ni(CO)(PPh_3)_3$, which was isolated and structurally characterized. Styrene dimerization is a major side reaction. Analysis of the reaction mechanism using density functional theory supported catalyst regeneration along with alkene formation as the most energetically demanding reaction steps.

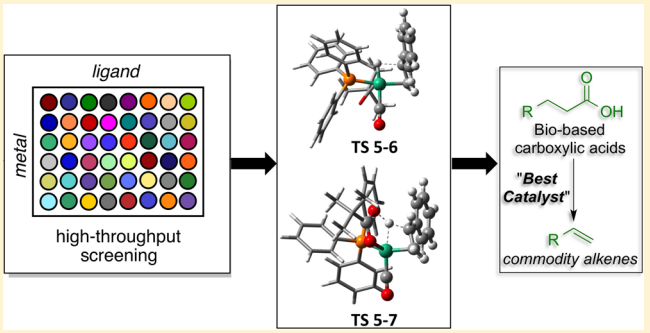

INTRODUCTION

In efforts to develop alternative routes to important polymers, new synthetic routes to high-volume and high-value monomers from renewable resources are key targets of current research.[1] In view of the prevalence of carboxylic acid functional groups in biomass-derived feedstocks, catalytic dehydrative decarbonylation to yield alkenes is an attractive approach for the synthesis of bioderived monomers (Scheme 1, inset). Building upon previous work using precious metals such as palladium,[2] rhodium,[2a] and iridium,[3] we recently reported the catalytic dehydrative decarbonylation of the renewable substrates hydrocinnamic acid (from cinnamaldehyde[4]), monoalkyl succinates (from biobased succinic acid), and 3-cyanopropanoic acid (from the amino acid glutamic acid[5]) to styrene, alkyl acrylates, and acrylonitrile, respectively, in high yields (>80%) using a palladium-phosphine catalyst in combination with pivalic anhydride (Scheme 1).[6] Related Pd catalysts with acetic anhydride as additive were used to convert fatty acids to terminal alkenes,[7] and in recent work, anhydride additive use was circumvented via Pd-catalyzed decarbonylation of *p*-nitrophenol esters.[8]

Although precious metals are effective catalysts, they are also expensive and rare. The use of inexpensive and readily available first-row transition metals is desirable, but there have been few reports of their use for the dehydrative decarbonylation of carboxylic acids. Recently, an iron-based catalyst was reported for the dehydrative decarbonylation of long chain fatty acids to terminal alkenes.[9] Using 10 mol % $FeCl_2$, 20−40 mol % of an added phosphine ligand, 100 mol % of the additives KI and acetic anhydride, and 20 psi of CO, high yields of terminal alkene products were obtained. In a noncatalytic route, alkenes were prepared in up to 56% yield from cyclic anhydrides and thioanhydrides using stoichiometric amounts of $(PPh_3)_2Ni(CO)_2$, $Fe_2(CO)_9$, or $(PPh_3)_3RhCl$; however, side reactions were observed for anhydrides containing abstractable hydrogens.[10] In addition, a low-valent nickel species generated in situ from $NiCl_2$ and zinc dust was shown to be effective for the

Scheme 1. Catalytic Dehydrative Decarbonylation of Carboxylic Acids to Alkenes (Inset) and Specific Example of Conversion of Hydrocinnamic Acid to Styrene Using Pivalic Anhydride as Additive

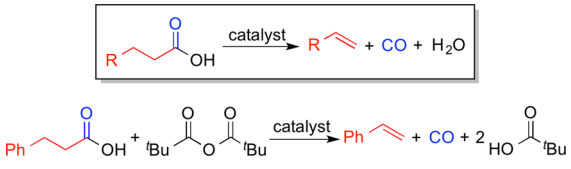

Received: May 24, 2016

DOI: 10.1021/acs.organomet.6b00415
Organometallics XXXX, XXX, XXX−XXX

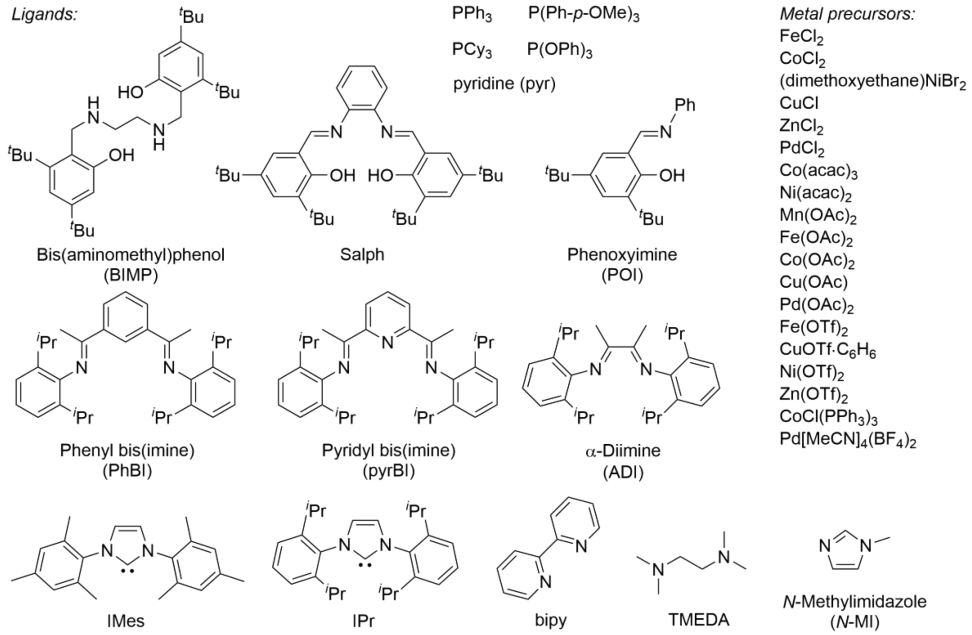

Figure 1. Ligands and metal precursors used in the first set of high-throughput screening reactions.

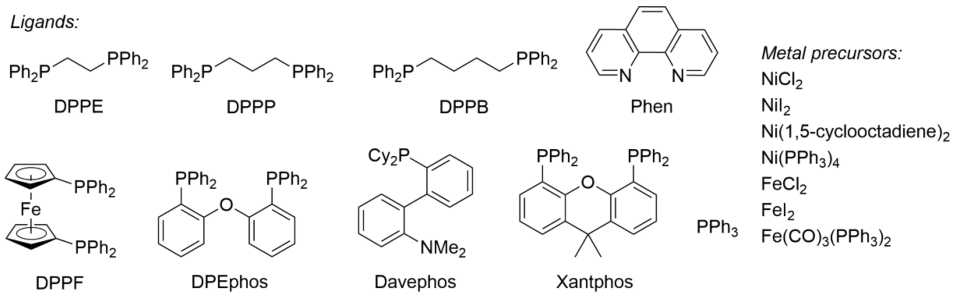

Figure 2. Ligands and metal precursors used in the second set of high-throughput screening reactions.

dehydrative decarbonylation of 2-pyridyl thioates.[11] The dehydrative decarbonylation of thioesters under similar conditions generated thioethers from unsaturated or aromatic substrates and alkenes from aliphatic substrates.[12] A disadvantage of these approaches is that 2-pyridyl thioates and thioesters must be prepared from the carboxylic acid prior to dehydrative decarbonylation. In the patent literature, nickel, cobalt, and iron precursors were reported to be effective dehydrative decarbonylation catalysts for carboxylic acids in the presence of KI or by using an iodide precursor, although conversions are lower than those observed with palladium or rhodium precursors.[13]

Inspired by literature precedent that suggested that the first-row metals could catalyze dehydrative decarbonylation reactions,[9−13] we were interested in screening a broad range of first-row transition metal−ligand combinations for the dehydrative decarbonylation of bioderived carboxylic acids. The conversion of hydrocinnamic acid to styrene was selected as a convenient and illustrative test case (Scheme 1). Herein we report the results of these studies, using a combination of high-throughput experimentation (HTE) and conventional batch catalyst assessment. HTE was used to expedite the initial discovery process, and conventional catalyst screening was used to explore active systems in more detail. Several new types of catalysts were identified for styrene production, their use in the dehydrative decarbonylation of fatty acids to produce long-chain alkenes was examined, and conditions that yielded high selectivity for linear alpha alkenes were discovered. Further experimental and theoretical studies provided mechanistic insights useful for guiding future catalyst development.

RESULTS AND DISCUSSION

Initial Catalyst Screening. A series of catalyst screening experiments was performed in order to identify effective metal precursors, ligands, and reaction conditions for the dehydrative decarbonylation of hydrocinnamic acid. All reagents were dispensed robotically. Metal−ligand combinations were screened in parallel in 96 × 1 mL arrays, and thin-layer chromatography (TLC) with UV light detection was used as a rapid, qualitative measure of reactivity due to its sensitivity (<1 mg). Validation of the high-throughput workflow as a suitable primary screen came from the observation of styrene formation by previously described[6] Pd/PPh_3 catalyst systems, which were included for validation of the workflow. Metal precursors and ligands screened in the first set of experiments are shown in Figure 1. Subsequent rounds of screening using the compounds shown in Figure 2 focused on the most promising Ni(II) and Fe(II) precursors as well as additional zerovalent compounds containing these metals under varying conditions (reaction time, ligand/metal loading, added CO or CO_2, varying amounts of KI), with monitoring of reaction products via GC in some cases. Detailed experimental descriptions and screening results are presented in the Supporting Information (Figures S1−S4,

DOI: 10.1021/acs.organomet.6b00415
Organometallics XXXX, XXX, XXX−XXX

Table 1. Effect of Nickel Precursor, KI, and PPh_3/Ni Ratio for Dehydrative Decarbonylation of Hydrocinnamic Acid[a]

entry	Ni precursor (mol %)	PPh_3 (mol %)	KI (mol %)	styrene yield (%)	ethylbenzene yield (%)	PivOH yield (%)
1	NiI_2 (5)	10	0	13	2.6	43
2	NiI_2 (5)	20	0	13	2.9	45
3	NiI_2 (10)	20	0	23	4.7	80
4	NiI_2 (10)	20	100	19	5.2	81
5	NiI_2 (10)	40	0	19	2.9	48
6	NiI_2 (10)	40	100	13	2.6	45
7	$Ni(PPh_3)_4$ (2)	8	100	7.0	0.4	7.4
8	$Ni(PPh_3)_4$ (5)	10	100	29	2.6	71
9	$Ni(PPh_3)_4$ (5)	20	100	13	1.1	25
10	$Ni(PPh_3)_4$ (10)	20	0	27	4.1	80
11	$Ni(PPh_3)_4$ (10)	20	100	30	3.2	81

[a]Reactions performed at 180 °C for 2 h, under a flow of N_2 or Ar using a distillation method. Styrene, ethylbenzene, and PivOH yields determined by GC-MS analysis of the distillate.

Table 2. Variation of Ni Source, Phosphine, and KI for Dehydrative Decarbonylation of Hydrocinnamic Acid[a]

entry	Ni precursor (mol %)	ligand (mol %)	KI mol %	time (h)	styrene yield (%)	ethylbenzene yield (%)	PivOH yield (%)
1	NiI_2 (10)	Davephos (20)	100	2	20	4.2	71
2	NiI_2 (10)	DPEphos (10)	100	2	21	2.5	61
3	NiI_2 (10)	DPPB (10)	100	2	34	8	81
4	NiI_2 (10)	DPPF (10)	100	2	15	2.7	58
5	NiI_2 (10)	DPPB (20)	100	24	28	6.9	83
6	$Ni(PPh_3)_4$ (5)	Davephos (10)	100	2	27	2.7	85
7	$Ni(PPh_3)_4$ (5)	DPEphos (5)	100	2	34	3.0	90
8	$Ni(PPh_3)_4$ (5)	DPPB (5)	100	2	23	2.4	60
9	$Ni(PPh_3)_4$ (5)	DPPF (5)	100	2	30	2.6	78
10	$Ni(PPh_3)_4$ (5)	DPPB (5)	0	2	24	4.5	44
11	$Ni(PPh_3)_4$ (5)	DPPB (5)	0	18	28	2.6	75

[a]Reactions performed at 180 °C, under a flow of N_2 or Ar using a distillation method. Styrene, ethylbenzene, and PivOH yields determined by GC-MS analysis of the distillate.

Tables S1−S8). While styrene formation was observed in many cases using a wide range of catalyst precursors, it should be noted that the TLC screen is very sensitive and can detect low-activity systems (1% conversion). Upon scale up, the best results were obtained using NiI_2 or Ni^0 precursors with a variety of phosphine ligands in a 2:1 P/Ni ratio. These systems were selected for follow-up studies. Ethylbenzene was identified as a coproduct, with a [styrene]/[ethylbenzene] ratio typically ranging from 1:1 to 4:1. Product formation was inhibited when the reaction was performed under CO or CO_2 pressure.

Batch Reactions of Hydrocinnamic Acid. In order to determine whether the general trends observed under high-throughput conditions were replicated under conventional batch conditions on a larger scale, reactions using the most promising Ni^{II} and Ni^0 precursors, NiI_2 and $Ni(PPh_3)_4$, and PPh_3 were run using a previously described experimental setup using 1.0 g (6.7 mmol) of hydrocinnnamic acid.[6] In agreement with the HTE results, the optimal ligand-to-metal ratio was 2:1 for both Ni^{II} and Ni^0 precursors, as seen in Table 1 (entries 3 and 8). Using NiI_2 as the metal precursor, the highest yield for styrene was found with 10 mol % NiI_2 and 20 mol % PPh_3 (23%, entry 3). Reactions using NiI_2 precursors generally required higher loadings, with an optimal loading of 10 mol %. For $Ni(PPh_3)_4$, an optimal loading of 5 mol % was determined; higher styrene yields were not observed at 10 mol % (entries 8 and 11). Addition of KI enhances styrene yield slightly for $Ni(PPh_3)_4$ (entries 10 and 11) and has minimal effect on the yield for NiI_2 (entries 3−6). Despite relatively low styrene yields, high yields of PivOH (70−80%) are observed for the catalyst conditions that generate the highest yields of styrene (entries 3, 4, 8, 10, and 11).

Using the optimized ligand-to-metal ratios and metal precursor loadings, the effect of ligand identity on the dehydrative decarbonylation efficiency and styrene yield was then explored (Table 2). Using NiI_2, the highest yields were obtained with DPPB (entry 3), with a styrene yield of 34%, although higher yields of ethylbenzene were also observed (8%). Allowing the reaction to proceed for 24 h did not afford an increase in styrene yield (entry 5). Although the bidentate phosphine DPPB gave the highest conversions, reactions with other bidentate phosphines did not show improved performance relative to PPh_3. Davephos (entry 1) and DPEphos (entry 2) resulted in comparable yields of styrene and PivOH to those observed with PPh_3, and DPPF (entry 4) had the lowest performance of the ligands tested with Ni(II). In general, $Ni(PPh_3)_4$ was more efficacious than NiI_2 with the ligands tested, although this may be due to catalysis by $Ni(PPh_3)_n$ intermediates. Addition of KI was found to enhance conversion and reduce ethylbenzene formation, although styrene yield was nearly unchanged (entries 8 and 10). Extending the reaction time to 18 h resulted in only a modest increase in styrene yields (entries 10 and 11).

From the data in Tables 1 and 2, a discrepancy between styrene and PivOH yields is evident; PivOH yields (or hydrocinnamic acid conversion) were higher than those of styrene in the distillate. These findings can be partly explained by the presence of styrene dimers and/or oligomers (such as the species shown in Figure 3) observed by GC-MS and NMR

DOI: 10.1021/acs.organomet.6b00415
Organometallics XXXX, XXX, XXX−XXX

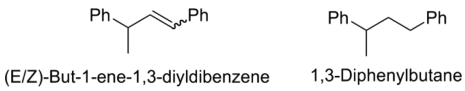

Figure 3. Styrene dimers isolated from the reaction mixture.

spectroscopy after the reaction had been worked up (Figures S5–S17). Metal hydride (M = Ni,[14] Pd,[15] Ir,[16] Ru[17]) species are known to facilitate the dimerization of styrene (and other alkenes) to give alkene- and alkane-containing dimers via a variety of mechanisms; typically, pathways analogous to those for alkene polymerization are invoked, although alternatives have been proposed.[15a,16,17]

Mechanistic Analysis of Hydrocinnamic Acid Reaction. *a. Experiments.* With the intent of gaining further understanding of the Ni-catalyzed dehydrative decarbonylation reaction and identifying the rate-limiting step, we performed a series of experiments designed to test various aspects of the generally accepted mechanism for the process (Scheme 2).[2b,6]

Scheme 2. Proposed Mechanism for Ni-Catalyzed Dehydrative Decarbonylation

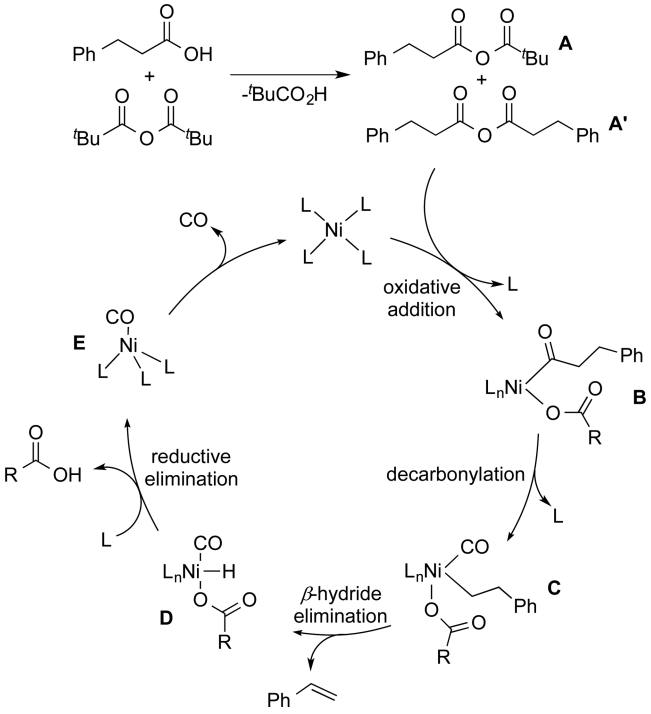

According to this mechanism, the carboxylic acid substrate reacts with the anhydride additive to yield new anhydrides (**A** and/or **A′**), which oxidatively add to the metal center to yield an acyl-carboxylate complex (**B**). Deinsertion to yield an alkyl complex (**C**) is then followed by β-hydride elimination, affording the product alkene and a metal hydride (**D**). Subsequent loss of carboxylic acid and CO regenerates the catalyst.

In initial experiments, we examined the activation of hydrocinnamic acid by the anhydride additive. The formation of the mixed anhydride, **A**, was observed to occur instantaneously upon combining equimolar amounts of hydrocinnamic acid and pivalic anhydride in benzene-d_6 at room temperature. However, as judged by ^{1}H NMR spectroscopy, it was generated only to the extent of ~21%, along with ~15% of the hydrocinnamic acid anhydride (**A′**), formed by reaction of **A** with another equivalent of hydrocinnamic acid (Scheme 3).

Scheme 3. Formation of Anhydrides A and A′

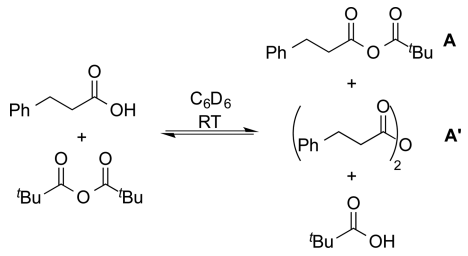

The ratio of the anhydride components in the mixture was found to be unchanged upon heating the mixture at 90 °C for 1 h or overnight. On the other hand, a higher proportion of the hydrocinnamic anhydride (**A′**, 51%; **A**, 35%) was generated under the reaction conditions (180 °C, 2 h, distillation of PivOH). These data suggest that under catalytic conditions the reaction mixture is enriched in **A′**.

In previous investigations of the feasibility of anhydride oxidative addition to low-valent phosphine-nickel complexes, facile oxidative addition was followed by decarbonylation to yield stable nickelalactones (from cyclic anhydrides) or aryl-nickel complexes (from aromatic carboxylic anhydrides).[18] We found that addition of 20 mol % $Ni(PPh_3)_4$ to the mixture formed upon adding pivalic anhydride to hydrocinnamic acid in benzene-d_6 at room temperature resulted in an instantaneous reaction, as indicated by an immediate color change from deep red-brown to a golden-yellow. Surprisingly, analysis of the resulting solution by ^{1}H NMR spectroscopy showed that styrene was generated under these conditions (20%, 1 turnover). This result indicates that alkene generation from the initially generated nickel-alkyl species is also facile at room temperature. The resulting [Ni-PPh_3] species showed a single resonance at δ 32.4 ppm in the ^{31}P NMR spectrum. Further turnovers were not observed at room temperature, but upon heating the reaction mixture at 100 °C for 1 h, the styrene yield increased to 30% (1.5 turnovers) with the generation of a second [Ni-PPh_3] species (^{31}P NMR peak at δ 33.5 ppm). However, no further increase in styrene yield was observed even upon continued heating for 2 days.

In order to probe the identity of the first [Ni-PPh_3] species (δ 32.4 ppm), an alternate route was sought that would generate a highly volatile alkene such as 1-propene, facilitating isolation of the Ni complex. Addition of stoichiometric amounts of $Ni(PPh_3)_4$ to a solution of *n*-butyric anhydride in benzene-d_6 at room temperature with stirring for 30 min resulted in the formation of 1-propene (75% by NMR) along with butyric acid and a species with a single peak in the ^{31}P NMR spectrum with the same chemical shift (δ 32.4 ppm) as that observed in the hydrocinnamic acid reactions. This species was isolated in 57% yield after recrystallization from a 1:1 mixture of toluene/pentane at −40 °C and was identified as $Ni(CO)(PPh_3)_3$ by X-ray crystallography (Figure S18 and Table S9).[19] The [Ni-PPh_3] species obtained after the second turnover was identified as $Ni(PPh_3)_2(CO)_2$ (^{31}P NMR = 33.5 ppm) by comparison with the ^{31}P NMR spectrum of an authentic sample purchased from Strem Chemicals. Similar [Ni-PPh_3]-containing species (^{31}P δ 32.4 and 33.5 ppm) were observed during experiments conducted starting with an independently prepared sample of hydrocinnamic anhydride

DOI: 10.1021/acs.organomet.6b00415
Organometallics XXXX, XXX, XXX−XXX

(A′) at 100 °C. Addition of other exogenous ligands {e.g., bidentate phosphines such as DPPE, DCYPE (1,2-bis(dicyclohexylphosphino)ethane), DPPF, or an N-heterocyclic carbene (IPr)} did not result in any improvements in styrene yield, and no further turnovers were obtained.

The aforementioned inability of the second complex, $Ni(PPh_3)_2(CO)_2$, to catalyze dehydrative decarbonylation of hydrocinnamic acid at 100 °C suggests that the regeneration of the active Ni(0) species (presumably by ligand loss) is the rate-limiting step in the sequence at lower temperatures. An independent catalytic run conducted using $Ni(CO)_2(PPh_3)_2$ as the catalyst (10 mol %) in the presence of DPPB (10 mol %) at 180 °C yielded 31% styrene (3 turnovers) in the distillate. Thus, at higher temperatures (180 °C), ligand loss is promoted and more turnovers can be attained.

We also examined the process by which the side products may be formed (ethylbenzene, styrene dimers). Ethylbenzene may be formed if Ni alkyl intermediate **D** is protonated by pivalic acid. Alternatively, it may be generated directly from hydrocinnamic acid by decarboxylation under the reaction conditions. When neat hydrocinnamic acid was heated in the presence of NiI_2 (20%), PPh_3 (40%), and KI (1 equiv) at 180 °C, ethylbenzene was obtained as the major product, albeit in low yield (9%), with an ethylbenzene to styrene ratio of 11:1. A similar study performed using $Ni(PPh_3)_4$ (20%) as the catalyst did not yield any deoxygenated products, suggesting that ethylbenzene formation takes place exclusively from the Ni(II) oxidation state. The feasibility of ethylbenzene originating from decarboxylation of hydrocinnamic acid is further supported by the observation that a higher amount of ethylbenzene is obtained in the distillate when half an equivalent of pivalic anhydride is used.

Styrene dimers are another side product observed in the reaction mixture. We hypothesize that the dimers result from subsequent Ni-catalyzed reactions of the initially formed styrene. Consistent with our hypothesis, when styrene or 4-methylstyrene was heated at 180 °C in the presence of $Ni(PPh_3)_4$ (10%) and pivalic acid (1−5 equiv relative to alkene), the respective dimeric products (Figure 3) were obtained in ∼40% yield (^{1}H NMR, identity confirmed by GC-MS). Multiple pathways for production of these compounds may be envisioned involving initial coordination of styrene to Ni(0)[20] and/or reaction with an intermediate Ni−H species (Scheme 4).[21] We are unable to distinguish among those pathways with the available evidence.

b. Theory. To shed light on the details of the hydrocinnamic acid dehydrative decarbonylation mechanism, we turned to quantum chemical calculations at the density functional level of theory (DFT; see Methods section for details). Since experiments suggest that $Ni(PPh_3)_4$ is one of the most efficient precatalysts (Table 1, entry 10), we explored the reaction as depicted in Scheme 5. All reported energies correspond to Gibbs free energies (kcal mol^{-1}) in butanoic acid (BA; chosen to mimic a solvent environment rich in pivalic acid) at 190 °C (463.15 K). The fully separated species $Ni(PPh_3)_4$, hydrocinnamic acid, and pivalic anhydride are used to define the zero of energy.

Scheme 4. Possible Routes for Generation of Styrene Dimers: (*i*) Styrene Coordination; (*ii*) Oxidative Coupling; (*iii*) β-Hydride Elimination; (*iv*) Reductive Elimination; (*v*) Protonation; (*vi*) Styrene Insertion

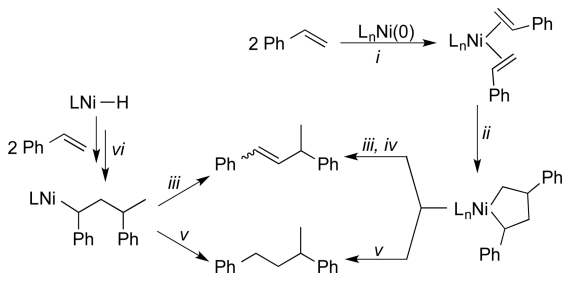

Scheme 5. Modeled Reaction for the Ni-Catalyzed Dehydrative Decarbonylation of A

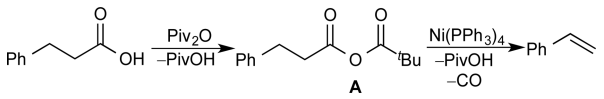

Following reaction of hydrocinnamic acid with pivalic anhydride to form the mixed anhydride **A**, the proposed mechanism[22] includes four elementary steps, namely, oxidative addition of the mixed anhydride to the metal,[23] decarbonylation of the acyl group, formation of styrene, and loss of CO to regenerate the catalyst (Scheme 2).

A complete reaction coordinate is shown in Figure 4 (L = PPh_3). Initially, one phosphine ligand dissociates from the [NiL_4] complex to generate a more stable trisphosphine species [NiL_3] with a free energy change of −7.7 kcal mol^{-1}. Subsequently, the mixed anhydride **A** coordinates to [NiL_3], forming **1** (2.2 kcal mol^{-1}). Dissociation of one phosphine ligand from [NiL_3] generates the active catalyst **2** (−0.3 kcal mol^{-1}), which undergoes oxidative addition. In the oxidative addition step (Scheme 6), C−O bond activation takes place via **TS2−3** at 9.3 kcal mol^{-1}. The resulting acyl−Ni intermediate (**B** in Scheme 2) can rearrange one phosphine ligand from its orientation *cis* in *cis*-**3** (−5.9 kcal mol^{-1}) to the more stable *trans* configuration in *trans*-**3** (−14.7 kcal mol^{-1}). Ligand loss from either *cis*- or *trans*-**3** leads to **4** (−7.3 kcal mol^{-1}), from which the decarbonylation step (Scheme 6) proceeds via **TS4−5** at 0.2 kcal mol^{-1} to generate alkylmetal intermediate **5** at −5.4 kcal mol^{-1} (**C** in Scheme 2).

Intermediate **5** can follow three alternative pathways leading to the formation of styrene (Scheme 7): β-hydride elimination followed by reductive elimination (Figure 4, blue line) and metal-assisted deprotonation via either the monophosphine (Figure 4, orange line) or phosphine-free (Figure 4, gray line) intermediates. Alternative pathways involving bisphosphine intermediates are less favored (see SI, Figure S19).

Considering first β-hydride elimination, TS structure **TS5−6** is found at 14.5 kcal mol^{-1}, which represents a free energy of activation of 29.2 kcal mol^{-1} relative to the preceding free energy sink *trans*-**3**. Owing to the basic nature of the pivalate group, intramolecular deprotonation of the C−H bond of the alkyl group by the pivalate ligand is also possible. A corresponding TS structure, **TS5−7**, was found at 11.1 kcal mol^{-1}, which reduces the free energy of activation to 25.8 kcal mol^{-1}. In this TS structure the metal center assists the proton transfer via a β-agostic interaction (Ni···H = 1.840 Å in **TS5−7**). The deprotonation pathway was also studied in the absence of the phosphine ligand. A phosphine-free metal-assisted deprotonation TS structure, **TS8−9**, is found at 10.5 kcal mol^{-1}, and its free energy of activation relative to *trans*-**3** is thus

DOI: 10.1021/acs.organomet.6b00415
Organometallics XXXX, XXX, XXX−XXX

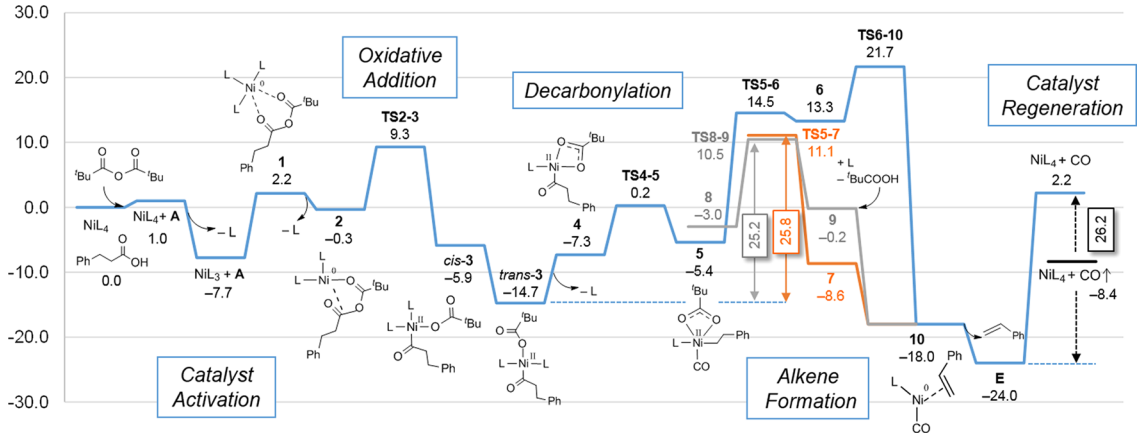

Figure 4. Gibbs free energy along the reaction coordinate (kcal mol^{-1}) for Ni-catalyzed dehydrative decarbonylation of hydrocinnamic acid.

Scheme 6. Oxidative Addition and Dehydrative Decarbonylation Steps[a]

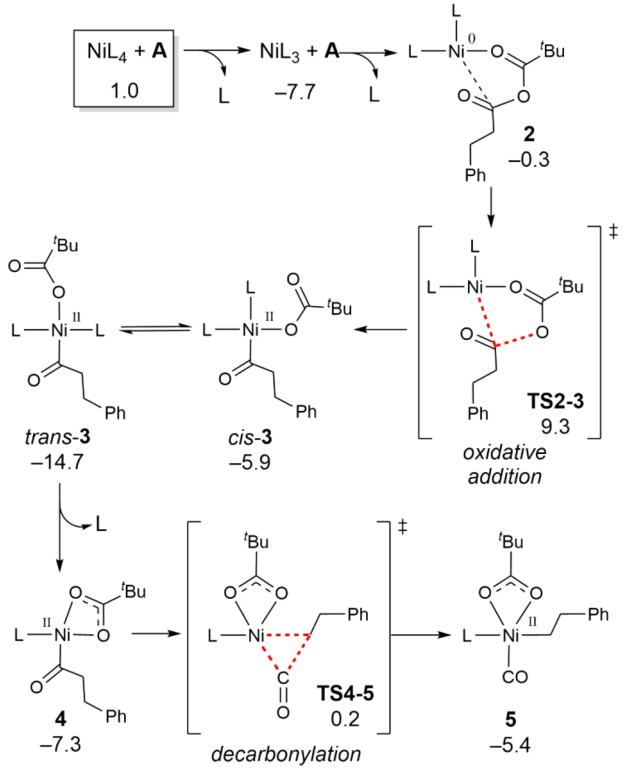

[a] ΔG_{BA} in kcal mol^{-1}.

Scheme 7. Alkene Formation Step[a]

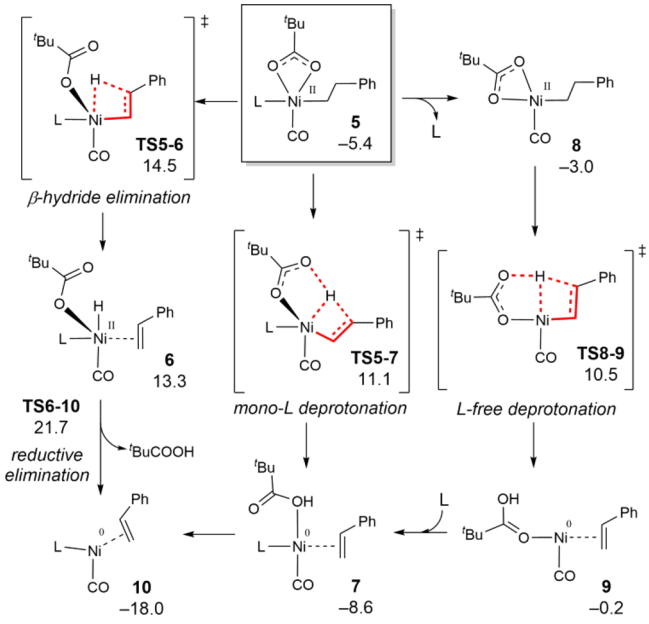

[a] ΔG_{BA} in kcal mol^{-1}.

25.2 kcal mol^{-1}. Thus, both monophosphine and phosphine-free deprotonation routes dominate reactivity.

After formation of the Ni-hydride intermediate **6** (**D** in Scheme 2) via β-hydride elimination, a subsequent reductive elimination step can occur via **TS6−10**, having a free energy of activation of 36.4 kcal mol^{-1} relative to free energy sink *trans*-**3**. However, this route to eliminate pivalic acid and intermediate **10** has a substantially higher barrier than do the deprotonation pathways, which by virtue of generating coordinated pivalic acid intermediate **7** or **9** directly, need only dissociate the carboxylic acid to generate **10**.

The final catalyst regeneration step requires recoordination of phosphine ligands and the dissociation of styrene and CO. Styrene release from **10** and recoordination of phosphine ligands generates complex [NiL$_3$(CO)] (**E** in Scheme 2) at −24.0 kcal mol^{-1} relative to initial reactants (i.e., the reaction to **E** is quite exergonic). The stability of **E** is consistent with its experimental observation in reaction mixtures (vide supra). To reenter the catalytic cycle, regeneration of [NiL$_4$] requires 26.2 kcal mol^{-1} (the free energy difference associated with replacing CO by PPh$_3$), and the *complete* reaction cycle is then predicted to be endergonic by 2.2 kcal mol^{-1}. However, that is a standard-state free energy associated with taking CO to have a standard-state pressure of 1 atm. Assuming that CO is swept from the system upon dissociation from Ni to a pressure of 10^{-5} atm, for instance, the free energy for a single turnover would then be −8.4 kcal mol^{-1}; that is, the catalytic cycle should proceed when CO is removed from the reaction medium.

For the proposed full reaction mechanism(s) for the Ni-catalyzed dehydrative decarbonylation of hydrocinnamic acid, the lowest standard-state free energy species in the cycle is carbonyl compound **E** ([NiL$_3$(CO)]) and the turnover-limiting free energy of activation may derive from the sum of the CO dissociation free energy (which is CO pressure dependent) and

DOI: 10.1021/acs.organomet.6b00415
Organometallics XXXX, XXX, XXX−XXX

the energy required to form intermediate **2** from regenerated catalyst. If CO pressure is kept sufficiently low, however, this sum may become sufficiently small to make the turnover-limiting free energy of activation correspond to that for alkene formation from *trans*-**3**, via either **TS5−7** (25.8 kcal mol^{-1}) or **TS8−9** (25.2 kcal mol^{-1}). This is fully consistent with the experimental observation that CO poisons the Ni catalyst through formation of the very stable [Ni−CO] species **E**. Along this line, a second catalytic cycle starting from **E** required larger activation barriers (see SI, Figure S20).

Our previous studies for Pd-catalyzed dehydrative decarbonylation of hydrocinnamic acid display a similar reactivity trend, albeit with larger activation barriers.[22] Regarding the catalyst regeneration, the bisphosphine Pd−acyl intermediate and [PdL$_3$(CO)] were close in energy, whereas the species [NiL$_3$(CO)] **E** is greatly favored and acts as a free energy sink.

Batch Reactions of Fatty Acids. We then investigated the reaction of the Ni catalysts with long-chain aliphatic carboxylic acids, many of which are derived from natural sources. It is particularly desirable to invent new methods for the synthesis of odd-numbered linear α-olefins (LAOs) by dehydrative decarbonylation of appropriate saturated fatty acids in view of the high cost of odd-numbered LAOs that are not accessible via ethylene oligomerization or ethenolysis of unsaturated fatty acids.[3b,7] Nonanoic acid was used as a convenient model substrate for the dehydrative decarbonylation of straight-chain aliphatic fatty acids, as its selective dehydrative decarbonylation would also yield industrially important 1-octene. We discovered that under the standard reaction conditions (Table 2, entry 3), nonanoic acid could be decarbonylated to octene(s) in 61% yield (Table 3, entry 1). In contrast to the reactions involving hydrocinnamic acid, analysis of the mixture did not show the presence of appreciable amounts of dimers in the reaction mixture. The nature of the phosphine ligand was observed to influence 1-octene (α-alkene) selectivity relative to other internal alkene isomers (Table 3, entries 2 + 3) using NiI$_2$ as the catalyst (Figure S21). Use of the Ni(0) catalysts, Ni(PPh$_3$)$_4$ and Ni(COD)$_2$, in the presence of added bidentate phosphine ligand was found to improve the reaction efficiency (yields 50−80%) and 1-octene selectivity (83−94%) significantly. The α-selectivity observed with our Ni(0)/L system is notable relative to other reported catalytic processes using Pd (80−99%), Fe (91−98%), or Ir (90−98%) catalysts.[2d,3,7,24] The yield of octene was adversely affected when a particularly strongly coordinating ligand such as 1,2-bis(dicyclohexylphosphino)-ethane (dcype, entry 9) was used. Increasing the ligand:Ni ratio (entry 8, L:Ni = 1.5) showed a slight improvement in the α-selectivity (94%) but at the expense of the overall alkene yield (56%). Lowering the catalyst loading (1 mol %, entry 11) resulted in reduced yields with a slight improvement in the α-selectivity (96%). In conclusion, we have identified Ni-based catalysts for the dehydrative decarbonylation of a representative long-chain fatty acid to a terminal α-alkene with high selectivity. Future computational efforts will focus on discerning the mechanism of the process and in particular the factors that underlie the high α-selectivity.

Table 3. Nickel-Catalyzed Dehydrative Decarbonylation of Nonanoic Acid[a]

entry	[Ni] (%)	ligand (%)	KI (%)	yield (%)	α-selectivity (%)
1	NiI$_2$ (10)	dppb (10)	100	61	37
2	NiI$_2$ (10)	PPh$_3$ (20)	100	63	61
3	NiI$_2$ (10)	DPEPhos (10)	100	55	52
4	Ni(PPh$_3$)$_4$ (5)	DPEPhos (5)		53	91
5	Ni(COD)$_2$ (5)	DPEPhos (5)		64	91
6	Ni(COD)$_2$ (5)	dppe (5)		50	83
7	Ni(COD)$_2$ (5)	dppf (5)		78	90
8	Ni(COD)$_2$ (5)	DPEPhos (7.5)		56	94
9	Ni(COD)$_2$ (5)	dcype (5)		4	76
10	Ni(COD)$_2$ (5)	XantPhos (5)		43	90
11	Ni(COD)$_2$ (1)	DPEPhos (1)		10	96

[a]Temperature: 180−190 °C, under a flow of N$_2$ using a distillation method, 2 h. Octene(s) yield and α-selectivity (1-octene) were determined by ^{1}H NMR spectroscopy using 1,3,5-trimethoxybenzene as an internal standard and confirmed by GC-MS.

SUMMARY AND CONCLUSIONS

Using a combination of high-throughput and conventional experiments, we determined that a combination of nickel precursors and arylphosphine ligands catalyze the dehydrative decarbonylation of hydrocinnamic acid to form styrene. Optimal ligand-to-metal ratios were determined to be 2:1, with a decrease in ligand-to-metal ratio resulting in a decreased yield of styrene. The reaction is inhibited by CO. A variety of phosphines were studied, and simple bidentate phosphines such as DPPB and DPEphos were found to increase the styrene yield, although they were only modestly better than PPh$_3$. A discrepancy between the observed styrene and pivalic acid yields has been attributed mostly to the generation of styrene dimers under the reaction condition. Mechanistic studies suggest that regeneration of the active [Ni-PPh$_3$] catalytic species via CO dissociation is the rate-limiting step in the sequence. Computational investigation of the catalytic mechanism supports these experimental results and identifies catalyst regeneration along with alkene formation as the most energy-demanding steps. The catalytic reaction conditions developed could be expanded to include other substrates. Specifically, we have demonstrated that fatty acids such as nonanoic acid can be efficiently decarbonylated to octene(s) under identical conditions. Ni(0) precursors in conjunction with bisphosphine ligands were found to be superior at achieving high α-selectivity (up to 94%) in these dehydrative decarbonylation reactions. Since octene is less reactive than styrene and has a lower boiling point, secondary dimerization reactions were not observed, resulting in high overall yields (up to 78%). Ongoing work in our laboratories is aimed at developing a more efficient process that would address (a) the need for high catalyst loading, (b) avoiding the use of an anhydride activator, and (c) achieving high α-selectivity in the decarbonylation of fatty acids.

EXPERIMENTAL SECTION

Materials and Methods. All experiments were carried out in an inert atmosphere unless otherwise noted. Metal precursors were purchased from Strem Chemicals or Sigma-Aldrich and used without further purification. Ni(PPh$_3$)$_4$ was synthesized according to literature procedures.[25] Pivalic anhydride was purchased from Aldrich and dried over molecular sieves. Hydrocinnamic acid purchased from Sigma-Aldrich was recrystallized from dry pentane and sublimed prior to use. KI was crushed in a mortar and pestle, then dried in an oven at 120 °C for 3 days prior to use. PPh$_3$ was recrystallized from ethanol prior to drying under vacuum. Bipy was recrystallized from hexane prior to drying under vacuum. TMEDA and *N*-methylimidazole were dried over CaH$_2$ and vacuum distilled prior to use. IMes,[26] IPr,[26] phenyl bis(imine),[27] pyridyl bis(imine),[28] α-diimine,[29] and bis-

DOI: 10.1021/acs.organomet.6b00415
Organometallics XXXX, XXX, XXX−XXX

(aminomethylphenol)[30] ligands were synthesized according to literature procedures. Phenoxyimine and salph ligands were prepared by condensation of 1 or 2 equiv of 3,5-di-*tert*-butylsalicylaldehyde, respectively, and aniline (for phenoxyimine) or *o*-phenylenediamine (for salph) in ethanol. All other organic compounds were purchased from Sigma-Aldrich or Strem and used as received. All GC-MS and GC experiments were conducted on an Agilent Technologies 7890A GC system with a 5975C VL MSD and an HP-5 ms silica column (30 m × 0.25 mm) or a Hewlett-Packard 6890 series gas chromatograph using a flame ionization detector and a Supelco 2-4304 beta-Dex 120 fused silica capillary column (30 m × 0.25 mm i.d., 0.25 μm film thickness). The standard method (with He as carrier gas) used for all runs involved an initial oven temperature of 50 °C (held for 2 min) followed by a 20 °C min^{-1} ramp to 70 °C (held for 6 min), followed by a final 20 °C min^{-1} ramp to 230 °C (held for 3 min).

High-Throughput Screening. All high-throughput experiments were performed using a Freeslate Core Module 3 (CM3) under a N_2 atmosphere in an MBraun glovebox. Reactions were performed in an Al rack containing 96 × 1 mL or 48 × 2 mL glass vials. Ligands were dispensed as stock solutions in THF or as neat liquids, and metal precursors were dispensed as solids or as solutions or slurries in THF. The reaction mixtures were allowed to complex for 1 h at room temperature, and then solvent was removed in vacuo using a ThermoSavant Speedvac vacuum centrifuge. Equimolar amounts of hydrocinnamic acid and of Piv_2O were added robotically. KI was added via automated solid addition. The plates were sealed and heated to either 100 or 180 °C and allowed to react for between 30 and 120 min, depending on the plate. At the end of the experiment, the arrays were removed from the glovebox, cooled, and analyzed for the presence of styrene using thin-layer chromatography (silica on glass as stationary phase, hexanes as mobile phase, imaged using UV light) or GC. TLC visualized with UV light is a very sensitive qualitative detection method for styrene; even very low amounts of styrene (<1 mg) can be detected.

Scale-up Reactions under $CO/CO_2/N_2$. In an inert-atmosphere glovebox, hydrocinnamic acid (1.0 g, 6.6 mmol or 0.50 g, 3.3 mmol), Piv_2O (1.35 mL, 6.66 mmol or 0.68 mL, 3.3 mmol), $Ni(PPh_3)_4$ (368 mg, 0.333 mmol or 154 mg, 0.139 mmol), and PPh_3 (175 mg, 0.666 mmol or 77 mg, 0.29 mmol) were added to a Fisher-Porter bottle, which was sealed and removed from the glovebox. The reactor was pressurized to 80 psi of CO or CO_2 gas or left at ambient pressure under N_2. The reaction was heated to 180 °C and allowed to react for 1.5 h. After the reaction time had finished, the reaction was cooled and diluted with 10 mL of hexanes. A 200 μL aliquot was taken for GC analysis and diluted to 1.5 mL using a solution of mesitylene in hexanes (201.2 mg in 100 mL of hexanes). Yields were determined from a calibration curve using mesitylene as an internal standard and are reported in Table 2.

Large-Scale (1 g) Dehydrative Decarbonylation Reactions. In a nitrogen-filled glovebox, hydrocinnamic acid (1.0 g, 6.7 mmol), Ni precursor (2−10 mol %), pivalic anhydride (1.35 mL, 6.66 mmol), KI (0−100 mol %), and phosphine ligand (5−20 mol %) were loaded into an oven-dried 10 mL round-bottom flask equipped with a Teflon stir bar. Not all of the reagents were soluble at room temperature, resulting in a heterogeneous mixture. The round-bottom flask was capped with a rubber septum, removed from the glovebox, and quickly attached to an oven-dried short-path distillation apparatus under a flow of argon gas. The reaction flask was lowered into a 160 to 170 °C oil bath and allowed to continue to heat until the oil bath reached 180 °C. Once the reaction mixture reached about 175 °C, it began to bubble, indicating loss of carbon monoxide. The reaction was allowed to proceed for the indicated time, during which time a distillate was collected. After 2 h, heating was ceased and the reaction was exposed to air. The distillate was analyzed using GC-MS, using mesitylene as an internal standard (representative GC-MS traces in Figures S5 and S6).

Workup of Reaction Mixture to Isolate Styrene Dimers. To the reaction with conditions in Table 2, entry 5, was added 200 mL of hexane to the reaction flask after it had cooled to room temperature to dissolve any hexane-soluble species. After stirring for 30 min, the hexane was separated from the hexane-insoluble components by filtration and the hexane was removed under vacuum. The residual material was analyzed by GC-MS (Figures S7−S11). To the hexane-insoluble material was added 125 mL of $CHCl_3$ with 100 mL of deionized water, and the mixture was allowed to stir for 30 min until everything dissolved in the chloroform/water phases. The layers were allowed to separate, and the yellow chloroform layer was washed once with 100 mL of NaOH (0.23 M), yielding a colorless solution, then once with 1 M aqueous HCl (20 mL). The chloroform was removed under vacuum to yield a yellow solid, which was also subjected to GC-MS analysis (Figures S12−S16). Both the hexane-soluble and hexane-insoluble GC-MS traces revealed that styrene dimers were the majority of the components present in the mixture.

Mass Balance in the Dehydrative Decarbonylation Reactions. A reaction was carried out using conditions mentioned in Table 2, entry 3, at 0.5 g scale of hydrocinnamic acid. The reaction was allowed to run for 30 min, by which time distillation had ceased. Both the distillate and residue from the reaction were analyzed directly by ^{1}H NMR spectroscopy using 1,3,5-trimethoxybenzene (1,3,5-TMB) as an internal standard. The distillate showed exclusively styrene (22%) and pivalic acid and minute traces of ethylbenzene. The residue was diluted with $CDCl_3$ (1 mL), and then an aliquot was analyzed using internal standard. The residue showed residual hydrocinnamic acid (20%), styrene (3%), and styrene dimer {(*E*/*Z*)-but-1-ene-1,3-diyldibenzene, 20%, *E*/*Z* = 7.6}. The saturated dimer, 1,3-diphenylbutane, was hard to identify/quantify in the ^{1}H NMR spectroscopy. By GC-MS, it was observed to be present only to the same extent as (*Z*)-but-1-ene-1,3-diyldibenzene. Based on residual hydrocinnamic acid quantified, the conversion of this reaction was 80%. The identified/quantified components account for ∼70% of the hydrocinnamic acid used for the reaction.

Mechanistic Studies. Inside a N_2-filled glovebox to a stirred solution of hydrocinnamic acid (0.020 g, 0.013 mmol) in benzene-d_6 (ca. 1 mL) was added pivalic anhydride (0.025 g, 0.013 mmol) and 1,3,5-trimethoxybenzene (0.004 g, 0.002 mmol). The mixture was transferred to a J-Young NMR tube, brought outside the box, and analyzed by ^{1}H NMR spectroscopy. The NMR tube was set in an oil bath preheated to 90 °C and then analyzed again after 1 h. Following this, it was then taken back inside the glovebox, and $Ni(PPh_3)_4$ (0.029 g, 0.002 mmol) was added to it. The reaction mixture was then allowed to stir for 2 min at room temperature, over which the color of the solution changed from deep red-brown to a yellow-green. The mixture was again sealed in the NMR tube and brought outside to be analyzed by NMR spectroscopy.

Dehydrative Decarbonylation of Butyric Anhydride. Inside a N_2-filled glovebox, $Ni(PPh_3)_4$ (0.029 g, 0.002 mmol) and 1,3,5-trimethoxybenzene (0.004 g, 0.002 mmol) were dissolved in benzene-d_6 (ca. 0.5 mL). The deep red-brown solution was transferred to a J-Young NMR tube, and a solution of *n*-butyric anhydride (0.004 g, 0.002 mmol) in benzene-d_6 (ca. 0.5 mL) was added. The mixture was agitated for even mixing, and within 5 min the color changed to yellow-green and it was analyzed by ^{31}P NMR. For isolation of the $Ni(CO)(PPh_3)_3$ species the reaction was performed using 0.135 g of $Ni(PPh_3)_4$ (0.12 mmol) and 0.019 g of *n*-butyric anhydride (0.12 mmol). $Ni(CO)(PPh_3)_3$ crystallized out of the reaction mixture (0.059 g, 57%).

Dehydrative Decarbonylation Reaction of Nonanoic Acid. In a nitrogen-filled glovebox, nonanoic acid (0.58 mL g, 3.3 mmol), Ni precursor (5−10 mol %), pivalic anhydride (0.67 mL, 3.3 mmol), KI (0−100 mol %), and phosphine ligand (5−20 mol %) were loaded into an oven-dried 10 mL round-bottom flask equipped with a Teflon stir bar. Not all of the reagents were soluble at room temperature, resulting in a heterogeneous mixture. The round-bottom flask was capped with a rubber septum, removed from the glovebox, and quickly attached to an oven-dried short-path distillation apparatus under a flow of argon gas. The reaction flask was lowered into a 160 to 170 °C oil bath and allowed to continue to heat until the oil bath reached 180 °C. Once the reaction mixture reached about 175 °C, it began to bubble, indicating loss of carbon monoxide. The reaction was allowed to proceed for the indicated time, during which time a distillate was collected. After 2 h, heating was ceased and the reaction was exposed

DOI: 10.1021/acs.organomet.6b00415
Organometallics XXXX, XXX, XXX−XXX

to air. The distillate was analyzed using ^{1}H NMR and GC-MS, using 1,3,5-TMB as an internal standard. Total alkene content in the distillate was estimated by using integrations of the alkene protons from the terminal and internal octene isomers vs 1,3,5-TMB. α-Selectivity was determined by comparing the ratio of terminal protons to internal protons. GC-MS analysis corroborated NMR analysis.

Computational Methods. All DFT[31] calculations were performed with Gaussian 09[32] using the M06-L functional.[33,34] Choice of M06-L was motivated by a survey of a variety of functionals compared to LPNO-CCSD[35] benchmark energies for dehydrative decarbonylation of hydrocinnamic acid in the system studied here but with Pd in place of Ni for the otherwise identical catalyst; M06-L was found to be optimal for that case.[22] Geometry optimizations for all minima and transition-state structures were carried out in the gas phase with the grid = ultrafine option for integral evaluations. Automatically generated density fitting permits cost-efficient computations by speeding up the evaluation of Coulomb integrals. The 6-31G(d,p) basis set[36] was used for H, C, O, and P with an additional diffuse function for O,[37] and the SDD[38] effective core potential and its associate double-ζ basis set was employed for Ni. All minima and transition states were confirmed by analytical vibrational frequency calculations at 463.15 K, and a single imaginary frequency was confirmed for each transition-state structure. Intrinsic reaction coordinates were checked to confirm that transition states connect to the corresponding reactants and products.[39] All frequencies below 50 cm^{-1} were replaced by 50 cm^{-1} when accounting for thermal contributions to vibrational partition functions.[40]

Solvation effects were incorporated through single point (SP) energy calculations using the SMD continuum solvation model.[41] Butanoic acid (ε = 2.85)[42] was chosen as a solvent to mimic the pivalic acid (ε = 2.98)[42] environment. In SP calculations, the SDD basis set with an additional f function[43] was used for Ni, and the 6-311++G(d,p) basis set[44] was used for the other atoms. All Gibbs free energies for all species (except as otherwise discussed for gaseous CO) were corrected by a factor of RT ln(38.0), corresponding to 3.3 kcal mol^{-1} for standard-state corrections from 1 atm gas to 1 M solution.

■ ASSOCIATED CONTENT

Supporting Information

The Supporting Information is available free of charge on the ACS Publications website at DOI: 10.1021/acs.organomet.6b00415.

Experimental details, representative GC and GC-MS spectra, tabulated HTE data, additional schemes, and Cartesian coordinates for all optimized species (PDF)

Crystallographic data for Ni(CO)(PPh$_3$)$_3$ (CIF)

■ AUTHOR INFORMATION

Corresponding Authors

*E-mail: lapointe@cornell.edu.
*E-mail: coates@cornell.edu.
*E-mail: cramer@umn.edu.
*E-mail: wtolman@umn.edu.

Author Contributions

§A. John, M. O. Miranda, and K. Ding contributed equally to the experimental work.

Notes

The authors declare no competing financial interest.

■ ACKNOWLEDGMENTS

We thank the National Science Foundation (Graduate Research Fellowship under Grant No. 00006595 to M.O.M.), the Center for Sustainable Polymers, a National Science Foundation supported Center for Chemical Innovation (CHE-1136607 and CHE-1413862), and the Department of Energy (DE-FG02-05ER15687) for financial support of this research. The authors acknowledge the Minnesota Supercomputing Institute (MSI) at the University of Minnesota for providing resources that contributed to the research results reported within this paper.

■ REFERENCES

(1) (a) Corma, A.; Iborra, S.; Velty, A. *Chem. Rev.* **2007**, *107*, 2411−2502. (b) Dapsens, P. Y.; Mondelli, C.; Pérez-Ramírez, J. *ACS Catal.* **2012**, *2*, 1487−1499. (c) Ragauskas, A. J.; Williams, C. K.; Davison, B. H.; Britovsek, G.; Cairney, J.; Eckert, C. A.; Frederick, W. J., Jr.; Hallett, J. P.; Leak, D. J.; Liotta, C. L.; Mielenz, J. R.; Murphy, R.; Templer, R.; Tschaplinski, T. *Science* **2006**, *311*, 484−489.

(2) (a) Miller, J. A.; Nelson, J. A.; Byrne, M. P. *J. Org. Chem.* **1993**, *58*, 18−20. (b) Foglia, T. A.; Barr, P. A. *J. Am. Oil Chem. Soc.* **1976**, *53*, 737−741. (c) Gooßen, L. J.; Rodríguez, N. *Chem. Commun.* **2004**, 724−725. (d) Le Nôtre, J.; Scott, E. L.; Franssen, M. C. R.; Sanders, J. P. M. *Tetrahedron Lett.* **2010**, *51*, 3712−3715.

(3) (a) Maetani, S.; Fukuyama, T.; Suzuki, N.; Ishihara, D.; Ryu, I. *Organometallics* **2011**, *30*, 1389−1394. (b) Ternel, J.; Lebarbé, T.; Monflier, E.; Hapiot, F. *ChemSusChem* **2015**, *8*, 1585−1592.

(4) (a) Lambert, M. A.; Moss, C. W. *J. Clin. Microbiol.* **1980**, *12*, 291−293. (b) Muller, A. J.; Bowers, J. S.; Eubanks, J. R. I.; Geiger, C. C.; Santobianco, J. G. U.S. Patent 5,939,581 1999.

(5) Le Nôtre, J.; Scott, E. L.; Franssen, M. C. R.; Sanders, J. P. M. *Green Chem.* **2011**, *13*, 807−809.

(6) Miranda, M. O.; Pietrangelo, A.; Hillmyer, M. A.; Tolman, W. B. *Green Chem.* **2012**, *14*, 490−494.

(7) Liu, Y.; Kim, K. E.; Herbert, M. B.; Fedorov, A.; Grubbs, R. H.; Stoltz, B. M. *Adv. Synth. Catal.* **2014**, *356*, 130−136.

(8) John, A.; Hogan, L. T.; Hillmyer, M. A.; Tolman, W. B. *Chem. Commun.* **2015**, *51*, 2731−2733.

(9) Maetani, S.; Fukuyama, T.; Suzuki, N.; Ishihara, D.; Ryu, I. *Chem. Commun.* **2012**, *48*, 2552−2554.

(10) (a) Trost, B. M.; Chen, F. *Tetrahedron Lett.* **1971**, *12*, 2603−2607. (b) Dauben, W. G.; Rivers, G. T.; Twieg, R. J.; Zimmerman, W. T. *J. Org. Chem.* **1976**, *41*, 887−889.

(11) Goto, T.; Onaka, M.; Mukaiyama, T. *Chem. Lett.* **1980**, *9*, 709−712.

(12) Wenkert, E.; Chianelli, D. *J. Chem. Soc., Chem. Commun.* **1991**, 627−628.

(13) (a) Suzuki, N.; Tahara, H.; Ishihara, D.; Danjo, H.; Mimura, T.; Ryu, I.; Fukuyama, T. U.S. Patent 2011/0190564A1 2011. (b) Suzuki, N.; Tahara, H.; Ishihara, D.; Danjo, H.; Ryu, I.; Fukuyama, T. U.S. Patent 2013/0296626A1, 2013.

(14) (a) Kron, T. E.; Lopatina, V. S.; Morozova, L. N.; Lebedev, S. A.; Isaeva, L. S.; Kravtsov, D. N.; Petrov, S. *Bull. Acad. Sci. USSR, Div. Chem. Sci.* **1989**, *38*, 703−707. (b) Yi, C.; Hua, R.; Zeng, H. *Catal. Commun.* **2008**, *9*, 85−88. (c) Faissner, R.; Huttner, G. *Eur. J. Inorg. Chem.* **2003**, *2003*, 2239−2244. (d) Jin, J.; RajanBabu, T. V. *Tetrahedron* **2000**, *56*, 2145−2151.

(15) (a) Peng, J.; Li, J.; Qiu, H.; Jiang, J.; Jiang, K.; Mao, J.; Lai, G. *J. Mol. Catal. A: Chem.* **2006**, *255*, 16−18. (b) Myagmarsuren, G.; Tkach, V. S.; Shmidt, F. K.; Mohamad, M.; Suslov, D. S. *J. Mol. Catal. A: Chem.* **2005**, *235*, 154−160. (c) Bedford, R. B.; Betham, M.; Blake, M. E.; Garcés, A.; Millar, S. L.; Prashar, S. *Tetrahedron* **2005**, *61*, 9799−9807. (d) Fanfoni, L.; Meduri, A.; Zangrando, E.; Castillon, S.; Felluga, F.; Milani, B. *Molecules* **2011**, *16*, 1804−1824.

(16) Bhalla, G.; Oxgaard, J.; Goddard, W. A.; Periana, R. A. *Organometallics* **2005**, *24*, 5499−5502.

(17) Lee, D. W.; Yi, C. S. *Organometallics* **2010**, *29*, 3413−3417.

(18) (a) Sano, K.; Yamamoto, T.; Yamamoto, A. *Chem. Lett.* **1983**, 115−118. (b) Sano, K.; Yamamoto, T.; Yamamoto, A. *Bull. Chem. Soc. Jpn.* **1984**, *57*, 2741−2747. (c) Fischer, R.; Nestler, B.; Schütz, H. *Z. Anorg. Allg. Chem.* **1989**, *577*, 111−114. (d) Döring, M.; Kosemund, D.; Uhlig, E.; Görls, H. *Z. Anorg. Allg. Chem.* **1993**, *619*, 1512−1518. (e) Fischer, R.; Walther, D.; Kempe, R.; Sieler, J.; Schönecker, B. *J. Organomet. Chem.* **1993**, *447*, 131−136.

DOI: 10.1021/acs.organomet.6b00415
Organometallics XXXX, XXX, XXX−XXX

(19) Isaeva, L. S.; Morozova, L. N.; Kravtsov, D. N. *Inorg. Chim. Acta* **1990**, *171*, 29−33.
(20) For an example of a styrene-coordinated Ni(0) complex see: Iglesias, M. J.; Blandez, J. F.; Fructos, M. R.; Prieto, A.; Álvarez, E.; Belderrain, T. R.; Nicasio, M. C. *Organometallics* **2012**, *31*, 6312−6316.
(21) A report of oxidative addition of benzoic anhydride to a Ni(0) center postulates a di-alkyl intermediate as the source of observed biphenyl from the stoichiometric reaction: Uhlig, E.; Nestler, B. *Z. Chem.* **1981**, *21*, 451−452.
(22) Ortuño, M. A.; Dereli, B.; Cramer, C. J. *Inorg. Chem.* **2016**, *55*, 4124−4131.
(23) (a) Gooßen, L. J.; Koley, D.; Hermann, H. L.; Thiel, W. *J. Am. Chem. Soc.* **2005**, *127*, 11102−11114. (b) Gooßen, L. J.; Koley, D.; Hermann, H. L.; Thiel, W. *Organometallics* **2006**, *25*, 54−67.
(24) Kraus, G. A.; Riley, S. *Synthesis* **2012**, *44*, 3003−3005.
(25) Ittel, S. D.; Berke, H.; Dietrich, H.; Lambrecht, J.; Harter, P.; Opitz, J.; Springer, W. *Inorganic Syntheses*; Springer, 1990; Vol. *28*, pp 98−104.
(26) Bantreil, X.; Nolan, S. P. *Nat. Protoc.* **2011**, *6*, 69−77.
(27) Nückel, S.; Burger, P. *Organometallics* **2000**, *19*, 3305−3311.
(28) Small, B. L.; Brookhart, M.; Bennett, A. M. A. *J. Am. Chem. Soc.* **1998**, *120*, 4049−4050.
(29) Johnson, L. K.; Killian, C. M.; Brookhart, M. *J. Am. Chem. Soc.* **1995**, *117*, 6414−6415.
(30) Tshuva, E. Y.; Gendeziuk, N.; Kol, M. *Tetrahedron Lett.* **2001**, *42*, 6405−6407.
(31) Cramer, C. J.; Truhlar, D. G. *Phys. Chem. Chem. Phys.* **2009**, *11*, 10757−10816.
(32) Frisch, M. J.; et al. *Gaussian 09*, Revision D.01; Gaussian, Inc.: Wallingford, CT, 2010.
(33) Zhao, Y.; Truhlar, D. G. *J. Chem. Phys.* **2006**, *125*, 194101.
(34) (a) Zhao, Y.; Truhlar, D. G. *Acc. Chem. Res.* **2008**, *41*, 157−167. (b) Zhao, Y.; Truhlar, D. G. *Chem. Phys. Lett.* **2011**, *502*, 1−13.
(35) Neese, F.; Hansen, A.; Liakos, D. G. *J. Chem. Phys.* **2009**, *131*, 064103.
(36) (a) Hehre, W. J.; Ditchfield, R.; Pople, J. A. *J. Chem. Phys.* **1972**, *56*, 2257−2261. (b) Francl, M. M.; Pietro, W. J.; Hehre, W. J.; Binkley, J. S.; Gordon, M. S.; DeFrees, D. J.; Pople, J. A. *J. Chem. Phys.* **1982**, *77*, 3654−3665.
(37) Clark, T.; Chandrasekhar, J.; Spitznagel, G. W.; Schleyer, P. *J. Comput. Chem.* **1983**, *4*, 294−301.
(38) Andrae, D.; Haeussermann, U.; Dolg, M.; Stoll, H.; Preuss, H. *Theor. Chim. Acta* **1990**, *77*, 123−141.
(39) (a) Hratchian, H. P.; Schlegel, H. B. *J. Chem. Phys.* **2004**, *120*, 9918−9924. (b) Hratchian, H. P.; Schlegel, H. B. *J. Chem. Theory Comput.* **2005**, *1*, 61−69.
(40) Ribeiro, R. F.; Marenich, A. V.; Cramer, C. J.; Truhlar, D. G. *J. Phys. Chem. B* **2011**, *115*, 14556−14562.
(41) Marenich, A. V.; Cramer, C. J.; Truhlar, D. G. *J. Phys. Chem. B* **2009**, *113*, 6378−6396.
(42) *CRC Handbook of Chemistry and Physics*, 95th ed.; CRC: Boca Raton, FL, 2014−2015.
(43) Ehlers, A. W.; Böhme, M.; Dapprich, S.; Gobbi, A.; Höllwarth, A.; Jonas, V.; Köhler, K. F.; Stegmann, R.; Veldkamp, A.; Frenking, G. *Chem. Phys. Lett.* **1993**, *208*, 111−114.
(44) (a) Krishnan, R.; Binkley, J. S.; Seeger, R.; Pople, J. A. *J. Chem. Phys.* **1980**, *72*, 650−654. (b) McLean, A. D.; Chandler, G. S. *J. Chem. Phys.* **1980**, *72*, 5639−5648.

DOI: 10.1021/acs.organomet.6b00415
Organometallics XXXX, XXX, XXX−XXX